

# An Experimental Investigation of a Date Seeds Hydro-acetonic Mixture Extract Inhibitor for Corrosion Inhibition of Carbon Steel in an Acidic Medium at High Temperatures.

Omar Anor<sup>1</sup>, Sara Lahmady<sup>1</sup>, Issam Forsal<sup>1,\*</sup> , Hafida Hanine<sup>2</sup>, Hamza Ourradi<sup>2</sup>, Anas Elharami<sup>1</sup>,

<sup>1</sup> Laboratory of Engineering and Applied Technologies, School of Technology, Beni Mellal, Morocco; hmed.anor@gmail.com (O.A.); sara1lhmedi@gmail.com (S.L.); forsalissam@yahoo.fr (I.F.); anaselharami@gmail.com (A.N.);

<sup>2</sup> Laboratory of Bioprocess and Biointerface, University Sultan Moulay Slimane, Faculty of Sciences and Technologies, Beni Mellal, Morocco; h.hanine@usms.ma (H.H.); Hamza.ourradi@usms.ma (H.O.);

\* Correspondence: forsalissam@yahoo.fr (I.F.);

Scopus Author ID 35434746700

Received: 8.06.2022; Accepted: 5.07.2022; Published: 10.07.2022

**Abstract:** The corrosion inhibition of carbon steel in 1.0M HCl by a hydro-acetonic mixture extract of date seeds (DS) was tested using potentiodynamic polarization (PDP) and electrochemical impedance spectroscopy (EIS). This work revealed that the mixture extract of DS studied acts as a mixed-type inhibitor, primarily controlling the anodic reaction. We found that the inhibition efficiency of DS increased with increasing concentration, reaching 94.164% at 2 g/L, and decreased with temperature. Increasing the concentration of the corrosion inhibitor enhances the surface coverage and formation of a protective film, which is proven by the results of immersion time. The mixture extract of date seeds (DS) was analyzed by the Fourier transform infrared (FTIR) technique.

**Keywords:** carbon steel; mixture extract of DS; EIS; PDP; FTIR; protective film.

© 2022 by the authors. This article is an open-access article distributed under the terms and conditions of the Creative Commons Attribution (CC BY) license (<https://creativecommons.org/licenses/by/4.0/>).

## 1. Introduction

Steel is often used in the chemical and petrochemical industries. Acid solutions, especially hydrochloric acid, are used for cleaning, pickling, descaling, and oil acidizing [1,2]. A hydrochloric acid solution is used more than others because it is more economical, effective, and less troublesome than mineral acids [3,4].

Thanks to the aggressiveness of acids, inhibitors are often applied to decrease the dissolution of metals [5,6]. As a result, assessing the corrosion phenomenon on metals, particularly different types of steel, and developing admirable methods are critical [7].

Different methods have been developed to control and prevent corrosion in many environments [8]. Using inhibitors is one of the most pragmatic strategies to prolong corrosion progress, which has become widespread recently [1,9]. Different organic and inorganic barriers have been studied to control the corrosion of metals [10,11]. Most organic compounds include nucleophiles like nitrogen, sulfur, oxygen atoms, heterocyclic compounds, and  $\pi$ -electrons, which allow adsorption on a metal surface [4,12]. However, most are expensive, poisonous, and contribute to environmental concerns. Unfortunately, the biological toxicity of these

inorganics, especially chromates and organophosphates, is pointing toward their environmentally harmful properties [13,14].

Recently, most attention has been focused on using natural inhibitors, for example, plant seeds [15], leaves, plant aqueous extracts, peels, fruits, pectin, lignin [16,17], oil extracts [18,19], plant alkaloids extracts [16], etc., as the most important and favorable compounds for the environment and humans. They have some advantages over chemical inhibitors, including being nonpoisonous, cheap, environmentally friendly, renewable, and readily available, which make them helpful [1,2].

The present work aims to study the efficient inhibition of the mixture of date seeds (DS) on the corrosion of carbon steel in 1 M HCl solution by using potentiodynamic polarization and electrochemical impedance spectroscopy (EIS) methods. The effects of temperature and immersion time are studied, and the FTIR is used to identify the functional groups present in the DS extract.

## 2. Materials and Methods

### 2.1. Extraction process.

The seeds of the eight cultivars under investigation (Majhoul, Bouslikhan, Boufgous, Khalt a, Lassian, Tadmamt, Bousthami, and Khalt z) were directly isolated from 10 kg of date fruit having the same origin, collected at the "Tamr stage" (full ripeness). The seeds were soaked in water, washed to get rid of any adhering date flesh, and then air-dried. Then, they were further dried at about 50 °C. Date pits of each variety were separately milled in a heavy-duty grinder and then preserved until analyses. The eight-date seed powder varieties were pooled to create a homogeneous sample. Then, 1g of this last was shaken with 250 mL of acetone-water (70:30, V/V) at room temperature for 12 hours. The acetonic mixture extract was centrifuged and then filtered, and the obtained filtrates were evaporated in a rotary evaporator at 40 °C [20,21]. Then, it was tested as an inhibitor of corrosion.

### 2.2. Materials.

The samples were cut into a rectangular shape of 0.9 cm × 0.8 cm, and then the specimens were sealed using an epoxy resin, leaving an exposed area of 0.72 cm<sup>2</sup>. A conventional three-electrode cell consisting of a carbon steel working electrode (WE), a platinum counter electrode (CE), and a saturated calomel electrode (SCE) serving as a reference electrode is used. Before each experiment, the surface of the working electrode was polished with 180, 220, 360, 400, 600,800,1000, 1200, 1500, and 2000 grit silicon carbide (SiC) abrasive papers. Then it is followed by washing with distilled water, degreased with acetone, dried at room temperature, and quickly immersed in an acidic solution. Hydrochloric acid (HCl) 1 M was prepared by diluting hydrochloric acid grad 37% from Sigma-Aldrich using distilled water. A volume of 100 mL of dilute hydrochloric acid was used to ensure proper immersion of the electrodes in the cylindrical Pyrex glass cell. The concentration range of employed inhibitors is from 0.5g/L to 2g/L in acidic media.

### 2.3. Electrochemical analysis.

The electrochemical Experiments of this work were carried out using an Origamaster potentiostat equipped with Origamaster 5 software. The typical three-electrode cell consisted

of a working electrode made of steel with an exposed area of 0.72 cm<sup>2</sup>, platinum as the counter electrode, and a saturated calomel electrode (SCE) as the reference electrode. The coupon was immersed in the corrosive solutions for 30 minutes before measurements to obtain a stable state open circuit potential (E<sub>ocp</sub>). Potentiodynamic polarization curves were acquired in the potential range of -750 to -100 mV relative to the (SCE) reference electrode at a scanning rate up to 1mV.S-1 starting from cathodic to anodic direction. To support PDP data, the Electrochemical Impedance was carried out at open circuit potential (E<sub>ocp</sub>) at the frequency range from 100 mHz to 1kHz by applying the signals of sine wave voltage of 10 mV peak to peak. The impedance diagrams are given as Nyquist representations. The results were fitted by using EC-Lab software. The effect of temperature on the inhibitor performance was controlled in a temperature range from 293K to 323 K. For reproducibility reasons, the measurements were repeated three times for each concentration and temperature.

#### 2.4. Fourier Transform Infrared Spectroscopy (FT-IR).

Extract of date seeds (DS) samples was analyzed using a Thermo Scientific Nicolet IS50 spectrophotometer equipped with a single reflection attenuated total reflectance (ATR) accessory in the range 400 – 4000 cm<sup>-1</sup> at a resolution of 16 cm<sup>-1</sup>. The spectra were analyzed using OMNIC software.

### 3. Results and Discussion

#### 3.1. Electrochemical experiments.

##### 3.1.1. Open-circuit potential (OCP).

Under free corrosion circumstances, the open-circuit potential was recorded versus time until the steady-state was reached. At 293 K, Figure 1 depicts the temporal variation of OCP of carbon steel immersed in 1M HCl medium without and with various inhibitor concentrations. Without the inhibitor, the potential rises for 30 minutes before stabilizing. This may be related to the ennoblement of the surface by the formation of a passivating film. In the presence of an inhibitor, the electrode potential tends to stabilize at -480 mV versus SCE for all inhibitor concentrations. This evolution (Figure 1) may be due to the modification of the interface, and a steady-state is reached after 30 min. After that, EIS and PDP measurements were performed.

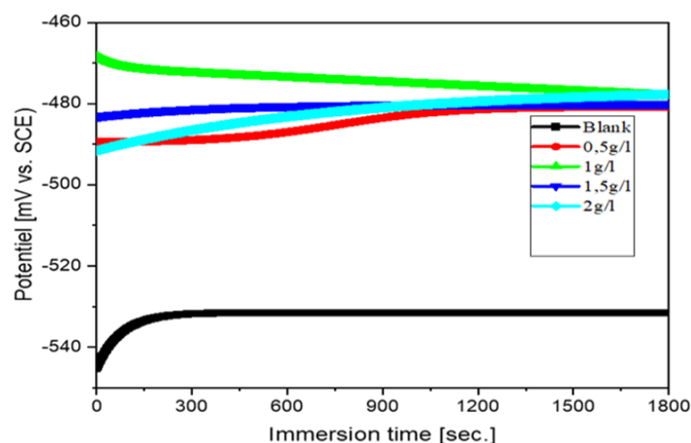


**Figure 1.** Variation of E<sub>0CP</sub>-time curves for carbon steel without and with inhibitor in 1 M HCl solution at 293K.

3.1.2. Polarization curve.

The polarization recorded in 1 M HCl solution without and with different concentrations of DS curves at 293 K is shown in Figure 2. Electrochemical parameters such as corrosion current density ( $j_{corr}$ ), corrosion potential ( $E_{corr}$ ), open-circuit potential ( $E_{ocp}$ ), Tafel slopes ( $\beta_a$ ,  $\beta_c$ ), and inhibition efficiency ( $\eta\%$ ) calculated using equation 1 are summarized in Table 1; it includes  $\theta$  the degree of surface coverage calculated by equation 2. [22].

$$\eta_{PDP} \% = \left( \frac{j_{corr}^0 - j_{corr}}{j_{corr}^0} \right) \times 100 \tag{1}$$

where  $j_{corr}^0$  and  $j_{corr}$  present the current densities without and with inhibitor, respectively.

$$\theta = 1 - \frac{j_{corr}}{j_{corr}^0} \tag{2}$$

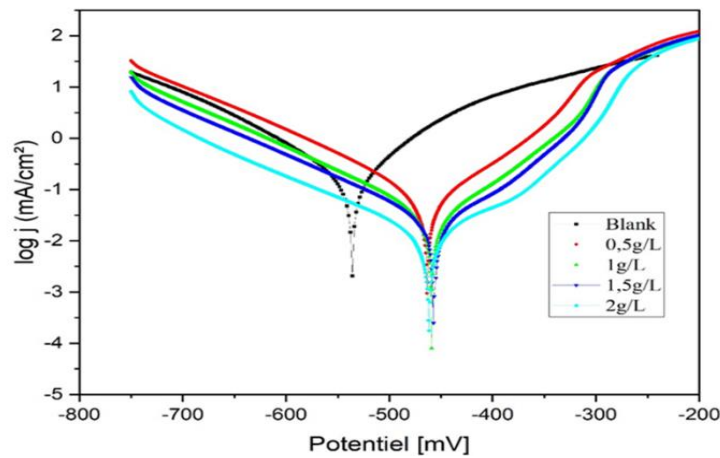


Figure 2. Polarization curves of Carbon steel in 1M HCl with presence and absence of different concentrations of DS.

Table 1. Polarization parameters for carbon steel in 1 M HCl in the presence and absence of DS extract.

Conc. (g/L)	$E_{ocp}$ (mV vs SCE)	$E_{corr}$ (mV vs SCE)	$j_{corr}$ ( $\mu\text{A}/\text{cm}^2$ )	$\beta_a$ (mV/dec)	$\beta_c$ (mV/dec)	$\eta_{PDP}(\%)$	$\theta$
Blank	-534.331	-536.1	217.6	83.5	-102.5		
0.5	-480.73	-463.3	103	71.5	-117.3	52.665	0.526
1	-478.76	-459	33.2	62.3	-107	84.743	0.847
1.5	-480	-456.4	25.8	59.4	-112.7	88.143	0.881
2	-477.76	-461.7	12.7	48.5	-119	94.164	0.941

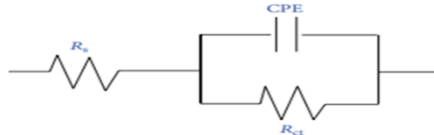
The addition of DS resulted in a displacement of  $E_{corr}$  towards a positive potential direction and a significant decrease in the anodic and cathodic current densities, as seen in Figure 2. This characteristic is due to its capacity to prevent hydrogen evolution and steel dissolution in HCl solution. Furthermore, parallel cathodic Tafel curves revealed that hydrogen evolution is activation-controlled and that the presence of this inhibitor has no effect on the reduction process of  $H^+$  ions [15].

Table 1 shows that increasing the inhibitor concentration resulted in a decrease in  $j_{corr}$  and, as a result, an increase in  $\eta$  (%), with the highest value, 94.16 %, at 2 g/L. Furthermore, the presence of the inhibitor affects the anodic Tafel slopes ( $\beta_a$ ). As a result, this inhibitor reduces the anode's partial current density, which may signify the inhibitor molecule adsorption on the steel surface. However, when compared to the blank, the addition of inhibitor resulted in a slight shift of corrosion potential towards positive values, with a maximum displacement of 79.7 mV, which is less than 85 mV, indicating that DS acts as a mixed-type corrosion inhibitor, primarily controlling the anodic reaction [23].

### 3.1.3. Electrochemical impedance spectroscopy (EIS).

The creation of an electric double layer with capacitance and resistance to charge transmission comes from the accumulation of solution species at the metal-solution interface during the corrosion process. As a result, this double layer may affect the mechanism and rate of electron transmission between cathodic and anodic sites on the metal surface [24]. The EIS approach is useful for determining the adsorption process, electrode kinetics, and surface properties [25].

In this investigation, the equivalent circuit shown in Figure 3 was employed to examine the EIS results. The equivalent circuit depicts monolayer inhibitor molecules' adsorption on the carbon steel surface.



**Figure 3.** Equivalent circuit model used to fit EIS data for carbon steel in 1M HCl.

The solution resistance, polarization resistance, and constant phase element are represented by  $R_s$ ,  $R_p$ , and  $CPE_{dl}$ , respectively. To better fit the experimental results with the proposed circuit model, the  $CPE_{dl}$  was used instead of a capacitor. However, according to equation 3, the double-layer capacitance ( $C_{dl}$ ) can provide a more dependable comparable circuit model [26].

$$C_{dl} = (Y_0 R_{ct}^n)^{\frac{1}{n}} \tag{3}$$

where  $n$  and  $Y_0$  are the exponential term (quantity of surface inhomogeneity) and the magnitude of admittance of the CPE.

In addition, the inhibitory efficiency  $\eta$  (%) of the DS was determined using equation 4 and polarization resistance data from EIS investigations [22].

$$\eta_{EIS} (\%) = \frac{R_{ct} - R_{ct0}}{R_{ct}} \times 100 \tag{4}$$

where  $R_{ct0}$  and  $R_{ct}$  are, respectively, charge transfer resistances in the absence and presence of DS at different concentrations.

Figure 4 shows Nyquist impedance diagrams obtained in 1 M hydrochloric acid without and with various inhibitor concentrations. The associated electrochemical parameters and fitted parameters are given in Table 2.

All impedance graphs shown in Figure 4 present semicircles associated with a single time constant, which demonstrates that charge transfer controls steel corrosion [27]. The presence of DS extract does not affect the corrosion mechanism of steel. The diameter of semicircles changes dramatically when DS extract is added to the corrosive media.

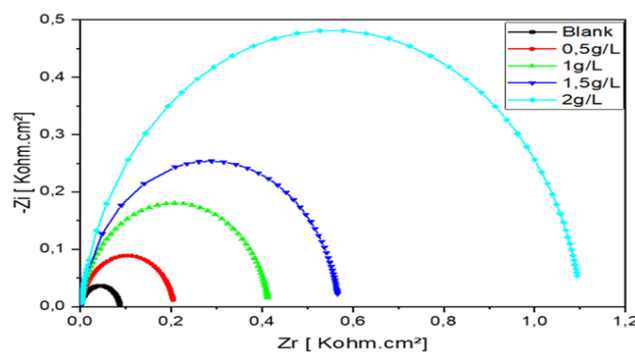


**Figure 4.** Nyquist plots for steel in 1 M HCl in the absence and presence of DS extract at 293K.

**Table 2.** Electrochemical impedance parameters obtained from EIS measurements for steel in 1 M HCl in the absence and presence of DS extract at 293 K.

Conc (g/L)	Re ( $\Omega \cdot \text{cm}^2$ )	Rct ( $\Omega \cdot \text{cm}^2$ )	Cdl ( $\mu\text{F} \cdot \text{cm}^{-2}$ )	CPE		$\eta_{\text{EIS}}$ (%)	$\theta$
				n	$Y_0 \times 10^{-6}$ ( $\Omega^{-1} \text{cm}^{-2}$ )		
Blank	0.777	87.78	210	0.886	330	---	---
0.5	1.153	206.2	215	0.908	286	57.43	0.574
1	0.379	415.1	96.34	0.911	128	78.13	0.781
1.5	1.470	569.1	77.92	0.928	97.46	84.57	0.845
2	1.632	1103	38.38	0.914	50.31	92	0.920

The concentration of DS extract causes its diameter to increase. Fitting experimental data into the analogous electrical circuit depicted in Figure 3 was used to examine Nyquist plots. It is made up of electrolyte resistance (Re), charge transfer resistance (Rct), and the diffusion effect index (n), which is close to 1, indicating excellent goodness of fit for the validation of the proposed equivalent circuit and the constant phase element (CPE) [28].

Table 2 shows that increasing the inhibitor reduces the double layer capacitance while increasing the charge transfer resistance. Rct increases when the local dielectric constant decreases and the thickness of the electrical double layer increases, implying the creation of a protective layer on the steel surface [29,30]. The increasing replacement of water molecules by adsorbed organic molecules is most likely to blame for the decline in double-layer capacitance [29].

Finally, it should be noted that the values of  $\eta$  (%), determined by the PDP and EIS are in good agreement.

### 3.1.4. Effect of temperature.

In general, the temperature significantly affects the corrosion process, as the corrosion rate increases as the temperature increases, resulting in a change in the adsorption mechanism of inhibitors. In addition, the active elements may degrade and/or rearrange [31].

The effect of this parameter on the corrosion rate of steel in the 1M HCl medium was investigated using polarization measurements at different temperatures ranging from 293 K to 323 K, with 2 g/L of DS extract (Figure 5). The electrochemical parameters of polarization curves are listed in Table 3.

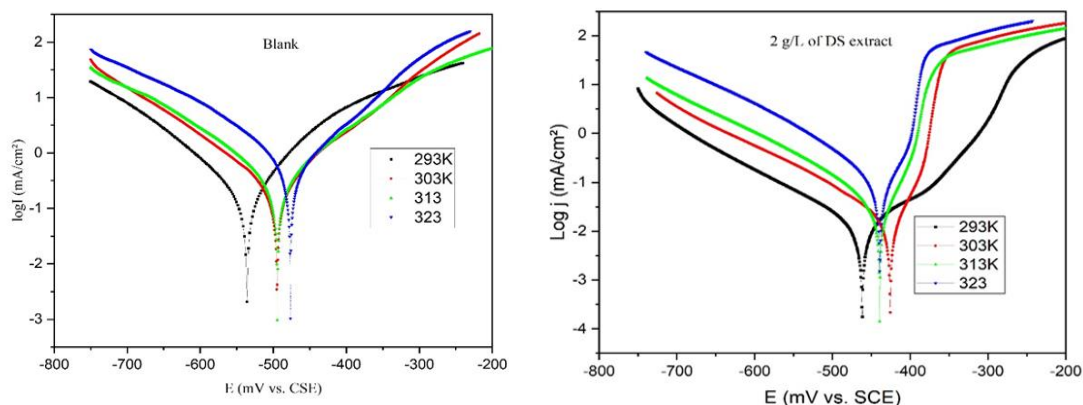


**Figure 5.** Polarization curves for steel in 1 M HCl with different temperatures.

The findings revealed that increasing the temperature decreased the corrosion rate very slightly in the presence of the inhibitor compared to the blank solution. This could be owing to the inhibitor molecules chemisorbing onto the steel surface [32]. The inhibitor adsorption

process is better understood by examining activation characteristics in the absence and presence of DS extract.

**Table 3.** Corrosion parameters obtained from potentiodynamic polarization of carbon steel in 1.0 M HCl with and without the addition of 2,5g/L of DS at different temperatures.

	T (K)	$I_{corr}$ ( $\mu\text{A}/\text{cm}^2$ )	$E_{corr}$ (mV vs SCE)	$\beta_a$ (mV/dec)	$\beta_c$ (mV/dec)	$\eta_{PDP}$ (%)
Blank	293	217.6	-536.1	83.5	-102.5	--
	303	277	-494.7	102	-116	--
	313	370	-494.4	108.6	-119.6	--
	323	602.1	-476.5	102.6	-103.3	--
2g/l of DS	293	12.7	-461.7	48.5	-119	94.19
	303	34.5	-429.9	23.9	-108	87.55
DS	313	39.1	-439.2	25.8	-106.5	89.43
	323	118	-439	24	-98.1	80.4

The classical Arrhenius equation, which analyzes the temperature dependence on corrosion current density, can also be used to determine the apparent activation energy (Equation 5) [18].

$$j_{corr} = A \exp\left(\frac{-E_a}{RT}\right) \tag{5}$$

where  $E_a$  is the apparent activation energy of the corrosion process,  $R$  is the universal gas constant ( $R = 8.314 \text{ J mol}^{-1} \text{ K}^{-1}$ ),  $T$  is the absolute temperature, and  $A$  is the Arrhenius pre-exponential factor.

Figure 6 shows the Arrhenius plot ( $\ln i_{corr}$  vs.  $1/T$ ) for carbon steel in a blank solution and the presence of 2g/L of DS at different temperatures.

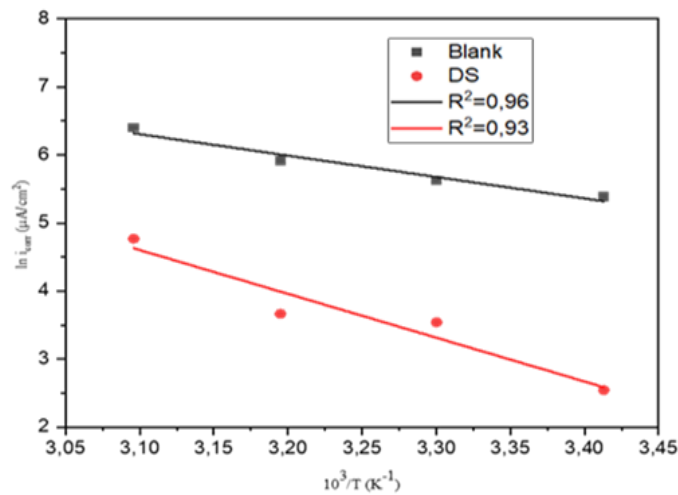


**Figure 6.** Arrhenius plot ( $\ln I_{corr}$  vs.  $10^3/T$ ) of C-steel in 1.0 M HCl solution with and without 2g/L of DS.

The activation energies were found to be 26.16 and 53.52 kJ/mol for 1.0 M HCl alone and in the presence of 2g/L of DS, respectively. The increase in activation energy after the addition of DS to 1.0 M HCl indicates an increase in the energy barrier for the corrosion of carbon steel [33,34]. Furthermore, the higher value of the apparent activation energy obtained in the presence of that inhibitor suggests that it could be physisorbed on the C-steel surface [35].

In addition, the inhibition efficiency of DS in acidic solution is compared to that of some other reported green corrosion inhibitors listed in Table 4. Although various corrosion inhibitors based on natural resources have been explored recently, most do not operate well at high temperatures. As shown in Table 4, at 50 °C, DS, on the other hand, performed admirably.

**Table 4.** Comparison of DS with other inhibitors.

Inhibitor	Concentration	Type of solution	Efficiency at room temperature (%)	Efficiency at high temperature	Type of adsorption	Reference
Cupressus arizonica fruit essential oil	0.5g/L of oil	1M HCl	93	77% at 50 °C	Mixed type inhibitor	[36]
Extract of Date Palm Seed	1400ppm	0,5M HCl	91	73% at 55 °C	Mixture adsorption	[14]
Mixture extract of Date seed	2g/L	1M HCl	94.16	80.4% at 50 °C	Physisorption	Present study
Quinoa seed	2g/L	1M HCl	98	86.1% at 40 °C	Physisorption	[37]

3.1.5. Effect of immersion time.

The evolution of the charge transfer resistance ( $R_{ct}$ ) of carbon steel at different immersion times (0.5H, 1H, 2H, 4H, 8 H, 10 H, 12 H, 24 H) in a 1M HCl medium in the absence and existence of the 2g/L of DS at temperature 293 K was monitored because of its importance in assessing the stability of the inhibitor behavior and the protective layer formed on the surface during the inhibition phenomenon. The electrochemical impedance diagrams obtained are shown in Figure 7. The associated electrochemical parameters and fitted parameters are given in Table 5.

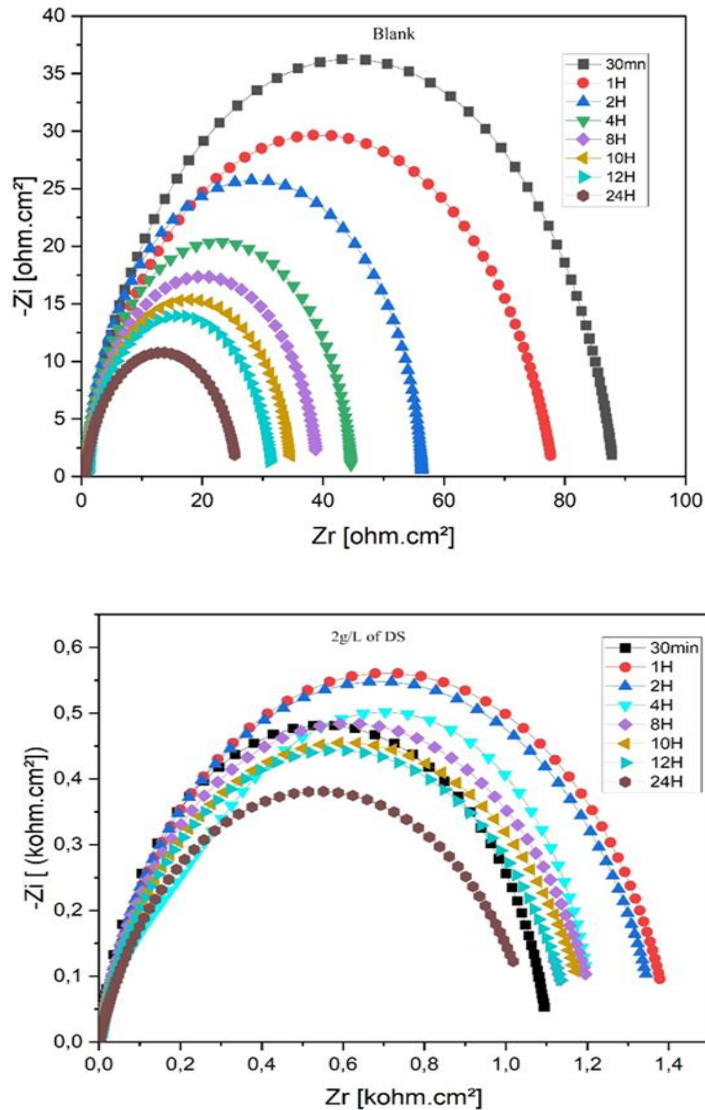


**Figure 7.** Nyquist plots for steel immersed in 1 M HCl in 1.0 M HCl solution with and without 2g/L of DS at different immersion times at 293 k.

After 1 h of immersion, a slight decrease in charge transfer resistance values is observed. This can be explained by the desorption of inhibiting molecules adsorbed to the metal surface for reasons related to the increase in surface roughness during exposure [38].

After that, the charge transfer resistance values remain constant at values identical to the initial value. These results highlight the stability of the adsorbed layer. Clearly, they show that the DS can be used as a temporary corrosion inhibitor of carbon steel in a 1M HCl acid medium.

**Table 5.** Electrochemical parameters for steel immersed in 1 M HCl in 1.0 M HCl solution with and without 2g/L of DS at different times of immersion at 293 k.

	Immersion time (H)	Rs ( $\Omega.cm^2$ )	Rct ( $\Omega.cm^2$ )	Cdl ( $\mu F.cm^{-2}$ )	n	Qdl ( $\mu\Omega^{-1} cm^{-2} S^n$ )	$\eta$ (%)
Blank	0.5	0.777	87.78	210	0.886	330	
	1	0.544	77.67	94.73	0.83	217	
	2	0.764	55.63	231	0.95	286	
	4	0.735	43.96	312	0.951	384	
	8	0.899	38.25	435	0.938	559	
	10	0.908	33.98	592	0.936	760	
	12	0.949	30.38	753	0.946	922	
	24	0.671	25.13	1510	0.902	2081	
2g/L of DS	0.5	1.632	1 103	38.38	0.914	50,31	92
	1	0.203	1379	53.78	0.911	73.54	94.37
	2	0.044	1 376	60.89	0.86	86.93	95.96
	4	0.168	1230	61.06	0.86	57.31	96.43
	8	0.034	1214	77.25	0.82	118	96.85
	10	0.536	1209	74.96	0.83	143	97.19
	12	0.0398	1169	71.97	0.83	110	97.4
	24	0.015	1078	112	0.8	177	97.67

### 3.2. FTIR analysis.

The FTIR spectrum for DS (Figure 8) shows a dominant peak at 3367  $cm^{-1}$  attributed to O–H stretching vibrations in hydroxyl groups [39]. The beaks at 2926 and 2856  $cm^{-1}$  are assigned to asymmetric C–H bands in methyl and methylene groups and symmetric C–H bands in methyl and methylene groups, respectively [19]. The band at 1607  $cm^{-1}$  may represent C=C or C=N vibrations in the aromatic region [40]. The peaks at 1521 and 1443  $cm^{-1}$  may be ascribed to C=C stretching of the aromatic skeletal mode [41,42].

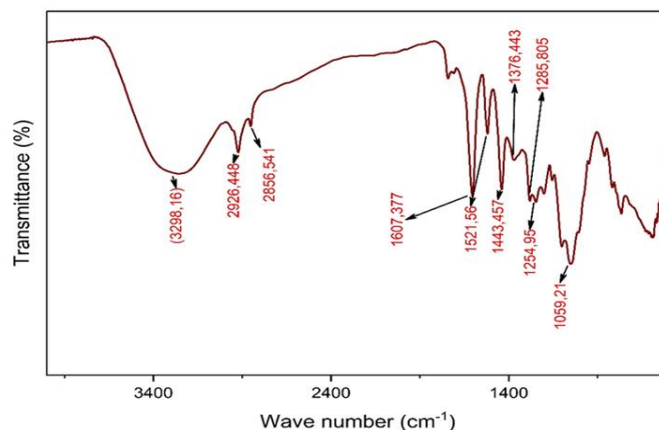


**Figure 8.** FTIR spectra of DS.

The peak at  $1376\text{ cm}^{-1}$  is due to the C–H stretching. The peak at  $1285$  and  $1254\text{ cm}^{-1}$  may be attributed to C–O–H deformation and C–O stretching of phenolics [19,41]. The band at  $1059\text{ cm}^{-1}$  may be attributed to C–O stretching vibration [41,42].

As a result, the findings revealed that the DS molecules include organic moieties rich in the aromatic ring, C-O, and O-H groups, which match the fundamental requirements of a good inhibitor.

#### 4. Conclusions

Various approaches were used to evaluate the adsorption and inhibitor effects of DS on the corrosion behavior of steel in 1 M HCl. The corrosion inhibition properties of hydro-acetonic mixtures of date seeds were tested in aggressive media and exhibited good inhibitory performance against carbon steel corrosion. The inhibition efficiency of carbon steel increases as the concentration of plant extract increases, and the corrosion process is controlled by charge transfer, according to impedance plots. The PDP curves revealed that the DES is a mixed-type corrosion inhibitor that largely controls the anodic process, correlating with the EIS findings.

#### Funding

This research received no external funding.

#### Acknowledgments

We thank all our colleagues.

#### Conflicts of Interest

The authors declare no conflict of interest.

#### References

1. Fazal, B.R.; Becker, T.; Kinsella, B.; Lepkova, K. A review of plant extracts as green corrosion inhibitors for CO<sub>2</sub> corrosion of carbon steel. *npj Materials Degradation* **2022**, *6*, 1-14, <https://doi.org/10.1038/s41529-021-00201-5>.
2. Kouache, A.; Khelifa, A.; Boutoumi, H.; Moulay, S.; Feghoul, A.; Idir, B.; Aoudj, S. Experimental and theoretical studies of Inula viscosa extract as a novel eco-friendly corrosion inhibitor for carbon steel in 1 M HCl. *Journal of Adhesion Science and Technology* **2022**, *36*, 988-1016, <https://doi.org/10.1080/01694243.2021.1956215>.
3. Hossain, N.; Asaduzzaman Chowdhury, M.; Kchaou, M. An overview of green corrosion inhibitors for sustainable and environment friendly industrial development. *Journal of Adhesion Science and Technology* **2021**, *35*, 673-690, <https://doi.org/10.1080/01694243.2020.1816793>.
4. Rathod, M.R.; Rajappa, S.K.; Praveen, B.M.; Bharath, D.K. Investigation of Dolichandra unguis-cati leaves extract as a corrosion inhibitor for mild steel in acid medium. *Current Research in Green and Sustainable Chemistry* **2021**, *4*, 100113, <https://doi.org/10.1016/j.crgsc.2021.100113>.
5. Abdallah, M.; Altass, H.M.; Al-Gorair, A.S.; Al-Fahemi, J.H.; Jahdaly, B.A.A.L.; Soliman, K.A. Natural nutmeg oil as a green corrosion inhibitor for carbon steel in 1.0 M HCl solution: Chemical, electrochemical, and computational methods. *Journal of Molecular Liquids* **2021**, *323*, 115036, <https://doi.org/10.1016/j.molliq.2020.115036>.
6. Fouda, A.S.; El-Desoky, H.S.; Abdel-Galeil, M.A.; Mansour, D. Niclosamide and dichlorphenamide: New and effective corrosion inhibitors for carbon steel in 1M HCl solution. *SN Applied Sciences* **2021**, *3*, 1-20, <https://doi.org/10.1007/s42452-021-04155-w>.
7. Alamiery, A.; Mahmoudi, E.; Allami, T. Corrosion inhibition of low-carbon steel in hydrochloric acid environment using a Schiff base derived from pyrrole: gravimetric and computational studies. *International*

- Journal of Corrosion and Scale Inhibition* **2021**, *10*, 749-765, <https://dx.doi.org/10.17675/2305-6894-2021-10-2-17>.
8. Kadhim, A.; Al-Amiery, A.A.; Alazawi, R.; Al-Ghezi, M.K.S.; Abass, R.H. Corrosion inhibitors. A review. *International Journal of Corrosion and Scale Inhibition* **2021**, *10*, 54-67, <https://dx.doi.org/10.17675/2305-6894-2021-10-1-3>.
  9. Chauhan, D.S.; Quraishi, M.A.; Qurashi, A. Recent trends in environmentally sustainable Sweet corrosion inhibitors. *Journal of Molecular Liquids* **2021**, *326*, 115117, <https://doi.org/10.1016/j.molliq.2020.115117>.
  10. Ma, I.A.W.; Ammar, S.; Kumar, S.S.A.; Ramesh, K.; Ramesh, S. A concise review on corrosion inhibitors: types, mechanisms and electrochemical evaluation studies. *Journal of Coatings Technology and Research* **2021**, *19*, 241-268, <https://doi.org/10.1007/s11998-021-00547-0>.
  11. Serdaroglu, G.; Kaya, S. Organic and Inorganic Corrosion Inhibitors: A Comparison. *Organic Corrosion Inhibitors: Synthesis, Characterization, Mechanism, and Applications* **2021**, 59-73, <https://doi.org/10.1002/9781119794516.ch4>.
  12. Nahlé, A.; Salim, R.; Hajjaji, F.E.; Ech-chihbi, E.; Titi, A.; Messali, M.; Kaya, S.; El Ibrahim, B.; Taleb, M. Experimental and Theoretical Approach for Novel Imidazolium Ionic Liquids as Smart Corrosion Inhibitors for Mild Steel in 1.0 M Hydrochloric Acid. *Arabian Journal of Chemistry* **2022**, 103967, <https://doi.org/10.1016/j.arabjc.2022.103967>.
  13. Soltani, N.; Tavakkoli, N.; Kashani, M.K.; Mosavizadeh, A.; Oguzie, E.E.; Jalali, M.R. Silybum marianum extract as a natural source inhibitor for 304 stainless steel corrosion in 1.0 M HCl. *Journal of Industrial and Engineering Chemistry* **2014**, *20*, 3217-3227, <https://doi.org/10.1016/j.jiec.2013.12.002>.
  14. Mohammed, N.J.; Othman, N.K.; Taib, M.F.M.; Samat, M.H.; Yahya, S. Experimental and Theoretical Studies on Extract of Date Palm Seed as a Green Anti-Corrosion Agent in Hydrochloric Acid Solution. *Molecules* **2021**, *26*, 3535, <https://doi.org/10.3390/molecules26123535>.
  15. Mostafatabar, A.H.; Bahlakeh, G.; Ramezanzadeh, B.; Dehghani, A.; Ramezanzadeh, M. A comprehensive electronic-scale DFT modeling, atomic-level MC/MD simulation, and electrochemical/surface exploration of active nature-inspired phytochemicals based on Heracleum persicum seeds phytoextract for effective retardation of the acidic-induced corrosion of mild steel. *Journal of Molecular Liquids* **2021**, *331*, 115764, <https://doi.org/10.1016/j.molliq.2021.115764>.
  16. Rani, B.E.A.; Basu, B.B.J. Green inhibitors for corrosion protection of metals and alloys: an overview. *International Journal of corrosion* **2012**, *2012*, 380217, <https://doi.org/10.1155/2012/380217>.
  17. Abdallah, M.; Altass, H.M.; Al Jahdaly, B.; Salem, M. Some natural aqueous extracts of plants as green inhibitor for carbon steel corrosion in 0.5 M sulfuric acid. *Green Chemistry Letters and Reviews* **2018**, *11*, 189-196, <https://doi.org/10.1080/17518253.2018.1458161>.
  18. Cherrad, S.; Alrashdi, A.A.; Lee, H.-S.; Lgaz, H.; Satrani, B.; Ghanmi, M.; Chaouch, A. Cupressus arizonica fruit essential oil: A novel green inhibitor for acid corrosion of carbon steel. *Arabian Journal of Chemistry* **2022**, *15*, 103849, <https://doi.org/10.1016/j.arabjc.2022.103849>.
  19. Oladipupo Kareem, M.; Edathil, A.A.; Rambabu, K.; Bharath, G.; Banat, F.; Nirmala, G.; Sathyanarayanan, K. Extraction, characterization and optimization of high quality bio-oil derived from waste date seeds. *Chemical Engineering Communications* **2021**, *208*, 801-811, <https://doi.org/10.1080/00986445.2019.1650034>.
  20. Al-Farsi, M.A.; Lee, C.Y. Optimization of phenolics and dietary fibre extraction from date seeds. *Food chemistry* **2008**, *108*, 977-985, <https://doi.org/10.1016/j.foodchem.2007.12.009>.
  21. Nehdi, I.; Omri, S.; Khalil, M.; Al-Resayes, S. Characteristics and chemical composition of date palm (Phoenix canariensis) seeds and seed oil. *Industrial crops and products* **2010**, *32*, 360-365, <https://doi.org/10.1016/j.indcrop.2010.05.016>.
  22. Tourir, R.; Cenoui, M.; El Bakri, M.; Touhami, M.E. Sodium gluconate as corrosion and scale inhibitor of ordinary steel in simulated cooling water. *Corrosion Science* **2008**, *50*, 1530-1537, <https://doi.org/10.1016/j.corsci.2008.02.011>.
  23. Mashuga, M.E.; Olasunkanmi, L.O.; Verma, C.; Sherif, E.-S.M.; Ebenso, E.E. Experimental and computational mediated illustration of effect of different substituents on adsorption tendency of phthalazinone derivatives on mild steel surface in acidic medium. *Journal of Molecular Liquids* **2020**, *305*, 112844, <https://doi.org/10.1016/j.molliq.2020.112844>.
  24. de Souza, F.S.; Spinelli, A. Caffeic acid as a green corrosion inhibitor for mild steel. *Corrosion science* **2009**, *51*, 642-649, <https://doi.org/10.1016/j.corsci.2008.12.013>.

25. Hernández, H.H.; Reynoso, A.M.R.; González, J.C.T.; Morán, C.O.G.; Hernández, J.G.M.; Ruiz, A.M.; Hernández, J.M.; Cruz, R.O. Electrochemical impedance spectroscopy (EIS): A review study of basic aspects of the corrosion mechanism applied to steels. *Electrochemical Impedance Spectroscopy* **2020**, 137-144, <https://doi.org/10.5772/intechopen.94470>.
26. Bentiss, F.; Jama, C.; Mernari, B.; El Attari, H.; El Kadi, L.; Lebrini, M.; Traisnel, M.; Lagrenée, M. Corrosion control of mild steel using 3, 5-bis (4-methoxyphenyl)-4-amino-1, 2, 4-triazole in normal hydrochloric acid medium. *Corrosion Science* **2009**, *51*, 1628-1635, <https://doi.org/10.1016/j.corsci.2009.04.009>.
27. Idouhli, R.; Koumya, Y.; Khadiri, M.; Aityoub, A.; Abouelfida, A.; Benyaich, A. Inhibitory effect of Senecio antephorbium as green corrosion inhibitor for S300 steel. *International Journal of Industrial Chemistry* **2019**, *10*, 133-143, <https://doi.org/10.1007/s40090-019-0179-2>.
28. Jacob, K.S.; Parameswaran, G. Corrosion inhibition of mild steel in hydrochloric acid solution by Schiff base furoin thiosemicarbazone. *Corrosion Science* **2010**, *52*, 224-228, <https://doi.org/10.1016/j.corsci.2009.09.007>.
29. Muthukrishnan, P.; Prakash, P.; Jeyaprabha, B.; Shankar, K. Stigmasterol extracted from Ficus hispida leaves as a green inhibitor for the mild steel corrosion in 1 M HCl solution. *Arabian Journal of Chemistry* **2019**, *12*, 3345-3356, <https://doi.org/10.1016/j.arabjc.2015.09.005>.
30. Prabakaran, M.; Kim, S.-H.; Kalaiselvi, K.; Hemapriya, V.; Chung, I.-M. Highly efficient Ligularia fischeri green extract for the protection against corrosion of mild steel in acidic medium: electrochemical and spectroscopic investigations. *Journal of the Taiwan Institute of Chemical Engineers* **2016**, *59*, 553-562, <https://doi.org/10.1016/j.jtice.2015.08.023>.
31. Idouhli, R.; Oukhrib, A.; Koumya, Y.; Abouelfida, A.; Benyaich, A.; Benharref, A. Inhibitory effect of Atlas cedar essential oil on the corrosion of steel in 1 m HCl. *Corrosion Reviews* **2018**, *36*, 373-384, <https://doi.org/10.1515/corrrev-2017-0076>.
32. Muthukrishnan, P.; Jeyaprabha, B.; Prakash, P. Adsorption and corrosion inhibiting behavior of Lannea coromandelica leaf extract on mild steel corrosion. *Arabian Journal of Chemistry* **2017**, *10*, S2343-S2354, <https://doi.org/10.1016/j.arabjc.2013.08.011>.
33. Verma, C.; Sorour, A.A.; Ebenso, E.E.; Quraishi, M. Inhibition performance of three naphthyridine derivatives for mild steel corrosion in 1M HCl: Computation and experimental analyses. *Results in Physics* **2018**, *10*, 504-511, <https://doi.org/10.1016/j.rinp.2018.06.054>.
34. Mishra, A.; Verma, C.; Lgaz, H.; Srivastava, V.; Quraishi, M.; Ebenso, E.E. Synthesis, characterization and corrosion inhibition studies of N-phenyl-benzamides on the acidic corrosion of mild steel: Experimental and computational studies. *Journal of Molecular Liquids* **2018**, *251*, 317-332, <https://doi.org/10.1016/j.molliq.2017.12.011>.
35. Ech-chihbi, E.; Nahlé, A.; Salim, R.; Oudda, H.; El Hajjaji, F.; El Kalai, F.; El Aatiaoui, A.; Taleb, M. An investigation into quantum chemistry and experimental evaluation of imidazopyridine derivatives as corrosion inhibitors for C-steel in acidic media. *Journal of Bio-and Tribo-Corrosion* **2019**, *5*, 1-18, <https://doi.org/10.1007/s40735-019-0217-9>.
36. Cherrad, S.; Alrashdi, A.A.; Lee, H.-S.; Lgaz, H.; Satrani, B.; Ghanmi, M.; Chaouch, A. Cupressus arizonica fruit essential oil: A novel green inhibitor for acid corrosion of carbon steel. *Arabian Journal of Chemistry* **2022**, *15*, 103849, <https://doi.org/10.1016/j.arabjc.2022.103849>.
37. Mobtaker, H.; Azadi, M.; Hassani, N.; Neek-Amal, M.; Rassouli, M.; Bidi, M.A. The inhibition performance of quinoa seed on corrosion behavior of carbon steel in the HCl solution; theoretical and experimental evaluations. *Journal of Molecular Liquids* **2021**, *335*, 116183, <https://doi.org/10.1016/j.molliq.2021.116183>.
38. Bouhlal, F.; Labjar, N.; Abdoun, F.; Mazkour, A.; Serghini-Idrissi, M.; El Mahi, M.; Lotfi, E.M.; Skalli, A.; El Hajjaji, S. Chemical and electrochemical studies of the inhibition performance of hydro-alcoholic extract of used coffee grounds (HECG) for the corrosion of C38 steel in 1M hydrochloric acid. *Egyptian Journal of Petroleum* **2020**, *29*, 45-52, <https://doi.org/10.1016/j.ejpe.2019.10.003>.
39. Nabili, A.; Fattoum, A.; Passas, R.; Elaloui, E. Extraction and characterization of cellulose from date palm seeds (Phoenix dactylifera L.). *Cellul. Chem. Technol* **2016**, *50*, 1015-1023.
40. Abu-Thabit, N.Y.; Judeh, A.A.; Hakeem, A.S.; Ul-Hamid, A.; Umar, Y.; Ahmad, A. Isolation and characterization of microcrystalline cellulose from date seeds (Phoenix dactylifera L.). *International Journal of Biological Macromolecules* **2020**, *155*, 730-739, <https://doi.org/10.1016/j.ijbiomac.2020.03.255>.

41. Nabili, A.; Fattoum, A.; Brochier-Salon, M.-C.; Bras, J.; Elaloui, E. Synthesis of cellulose triacetate-I from microfibrillated date seeds cellulose (*Phoenix dactylifera* L.). *Iranian Polymer Journal* **2017**, *26*, 137-147, <https://doi.org/10.1007/s13726-017-0505-5>.
42. Umoren, S.A.; Solomon, M.M.; Obot, I.B.; Suleiman, R.K. Comparative studies on the corrosion inhibition efficacy of ethanolic extracts of date palm leaves and seeds on carbon steel corrosion in 15% HCl solution. *Journal of adhesion science and Technology* **2018**, *32*, 1934-1951, <https://doi.org/10.1080/01694243.2018.1455797>.